Available online at www.sciencedirect.com

SCIENCE DIRECT

Remote Sensing of Environment 98 (2005) 225 – 236

Remote Sensing of Environment

www.elsevier.com/locate/rse

Vegetation water content estimation for corn and soybeans using spectral indices derived from MODIS near- and short-wave infrared bands

Daoyi Chen [a,*], Jingfeng Huang [b], Thomas J. Jackson [c]

[a] *Department of Engineering, University of Liverpool, Liverpool, L69 3BX, UK*
[b] *School of Mechanical, Aerospace and Civil Engineering, The University of Manchester, Manchester, M60 1QD, UK*
[c] *Hydrology and Remote Sensing Laboratory, Agricultural Research Service, US Department of Agriculture, USA*

Received 29 March 2005; received in revised form 24 June 2005; accepted 10 July 2005

Abstract

The estimation of vegetation water content (VWC) over a crop-growing period was performed using the near-infrared (NIR) and short-wave infrared (SWIR) bands of the Terra-MODerate Resolution Imaging Spectroradiometer (Terra-MODIS). The study was conducted in Iowa, USA as part of the Soil Moisture Experiments 2002 (SMEX02). Due to the moderate resolution of MODIS data, the removal of mixed pixels was important in order to meet accuracy estimation requirements of potential applications. MODIS-derived reflectance for the NIR and SWIR bands over corn and soybeans fields was validated using atmospherically corrected Landsat Thematic Mapper (TM)/Enhanced Thematic Mapper (ETM) data. All possible combinations of the 7 MODIS bands were used to construct VIs. The performance of each combination was evaluated by computing their correlations with corn VWC. The Normalized Difference Vegetation Index (NDVI) and the Normalized Difference Water Index (NDWI) were found to be the best candidates. In this study, it was observed that the MODIS SWIR-based VI for corn saturated at a later date than NDVI. A similar late saturation was observed for soybeans with a lag of about 10 days. Linear relationships between the SWIR-based VI and VWC were developed using the MODIS data and ground measured VWC. MODIS-derived Normalized Difference Water Indices (NDWI) using SWIR (1640 nm) or SWIR (2130 nm), namely $NDWI_{1640}$ or $NDWI_{2130}$, all showed potential in estimating VWC. Additional testing of this approach could result in a robust technique for estimating VWC for specific crops.

Keywords: MODIS; NDVI; NDWI; Landsat; SMEX02; Vegetation water content

1. Introduction

For three decades the Normalized Difference Vegetation Index (NDVI) has been used to estimate vegetation water content (VWC) with limited success. The limitation is related to its saturation when vegetation coverage is dense. For example, the saturation of NDVI at high leaf area index (LAI) was reported in Gamon et al. (1995) and Chen and Brutsaert (1998). NDVI is based on the red (RED) and near-infrared (NIR) bands, which are located in the strong chlorophyll absorption region and high reflectance plateau of vegetation canopies respectively. Therefore, NDVI represents chlorophyll rather than water content (Gamon et al., 1995; Gao, 1996).

A potentially better way of estimating VWC is to use indices based on the longer wavelength reflective infrared

Abbreviations: 6S, Second simulation of the satellite signal in the solar spectrum; AVIRIS, Airborne Visible/Infrared Imaging Spectrometer; DOY, Day of Year; EWT, Equivalent Water Thickness; LAI, Leaf Area Index; LDOPE, MODIS Land Data Operational Product Evaluation; Landsat, Landsat Thematic Mapper/Enhanced Thematic Mapper; MODIS, Moderate Resolution Imaging Spectroradiometer; NDVI, Normalized Difference Vegetation Index; NDWI, Normalized Difference Water Index; NIR, Near-infrared; PSF, Point Spread Function; QA, Quality Assessment; SMEX02, Soil Moisture Experiments in 2002 (http://hydrolab.arsusda.gov/smex02/); SWIR, Short-wave Infrared; VI, Vegetation Index; VIS, Visible; VWC, Vegetation Water Content; VWR, Vegetation Water Ratio; WC, Walnut Creek Watershed.

* Corresponding author. Tel.: +44 161 200 4618; fax: +44 161 200 4646.
E-mail addresses: daoyi.chen@manchester.ac.uk (D. Chen), j.huang-2@postgrad.manchester.ac.uk (J. Huang), tjackson@hydrolab.arsusda.gov (T.J. Jackson).

0034-4257/$ - see front matter © 2005 Elsevier Inc. All rights reserved.
doi:10.1016/j.rse.2005.07.008

range (1240–3000 nm), for example, the short-wave infrared (SWIR) reflectance (1300–2500 nm). Using satellite spectrometers and the Airborne Visible/Infrared Imaging Spectrometer (AVIRIS) data, it has been found that vegetation indices (VI) based upon NIR and SWIR are better than those employing VIS and NIR when retrieving leaf water content information (Ceccato et al., 2001; Gao, 1996; Gao & Goetz, 1995; Hunt & Rock, 1989; Hunt & Running, 1990; Rollin & Milton, 1998; Serrano et al., 2000; Sims & Gamon, 2002; Ustin et al., 1997). The advantage of using SWIR data was also demonstrated in modeling studies (Ceccato et al., 2001; Fourty & Baret, 1997; Tucker, 1980; Ustin et al., 1997; Zarco-Tejada et al., 2003). Studies using operational satellites also provided evidence on the benefits of the SWIR bands (Ceccato et al., 2002b; Chen et al., 2003; Jackson et al., 2004). Compared to NDVI, it has been found that saturation of SWIR-based spectral index occurs later (Roberts et al., 1997). To date, the MODIS SWIR bands have not been fully evaluated for the estimation of VWC.

Although it has a higher spatial resolution than MODIS, the utilization of Landsat TM/ETM (referred to as Landsat hereafter) in VWC mapping is limited by its infrequent temporal coverage and cost. In contrast, MODIS data is free and available daily (every other day at the equator) with moderate resolution and narrower reflected bandwidth ranges. The resolution of MODIS is at 250 m for bands 1–2 (centered at 648 and 858 nm) and 500 m for bands 3–7 (centered at 470, 555, 1240, 1640, and 2130 nm).

A vegetation index that may provide VWC information is typically a simple ratio utilizing data from two wavelengths: a reference wavelength where the water absorption coefficient is low and a measurement wavelength where water absorption is moderate or high and the penetration depth into the canopy is maximized (Gao, 1996).

The NIR (858 nm) band has been identified as a good choice for reference band in previous studies (Bull, 1991; Gao, 1996; Sims & Gamon, 2002; Penuelas et al., 1993; Roberts et al., 1997). It is suitable for normalization because it is relatively insensitive to vegetation water content changes in comparison with the longer wavelengths of NIR and SWIR bands as well as its relatively better canopy penetration ability in relation to visible bands. In order to establish physically meaningful vegetation index for VWC estimation, the SWIR bands with strong water absorption features were used in this study. The penetration of the bands into the canopy can be shown in the soil effect from soil background interaction, especially when there are sparsely vegetative conditions. Additionally, the sensitivity study conducted by Ceccato et al. (2002a) showed that more than 50% of the changes in the SWIR bands are due to the absorption caused by leaf equivalent water thickness (EWT). Pu et al. (2003) also demonstrated the increase of the reflectance at SWIR bands which are the main feature in water absorption bands.

In other studies using Landsat data, such as Chen et al. (2003) and Jackson et al. (2004), the SWIR (1550–1750 nm) was used, which was supported from the work of Tucker (1980). The SWIR (1640, 2130 nm) bands are water absorption dominated and as a result they are sensitive to VWC variations. In the current investigation the performance of vegetation indices based upon various band combinations in estimating VWC is examined.

Based on the discussions above, a set of NDWI functions using the NIR and the SWIR bands is evaluated in this study for VWC estimation:

$$\mathrm{NDWI}_{1640} = (\mathrm{NIR}_{858\ \mathrm{nm}} - \mathrm{SWIR}_{1640\ \mathrm{nm}}) / (\mathrm{NIR}_{858\ \mathrm{nm}} + \mathrm{SWIR}_{1640\ \mathrm{nm}}) \quad (1)$$

$$\mathrm{NDWI}_{2130} = (\mathrm{NIR}_{858\ \mathrm{nm}} - \mathrm{SWIR}_{2130\ \mathrm{nm}}) / (\mathrm{NIR}_{858\ \mathrm{nm}} + \mathrm{SWIR}_{2130\ \mathrm{nm}}) \quad (2)$$

In addition, for comparison purposes, a NDVI is also utilized:

$$\mathrm{NDVI} = (\mathrm{NIR}_{858\ \mathrm{nm}} - \mathrm{RED}_{648\ \mathrm{nm}}) / (\mathrm{NIR}_{858\ \mathrm{nm}} + \mathit{RED}_{648\ \mathrm{nm}}). \quad (3)$$

Based upon previous studies and theoretical considerations, the indices described above have been expected to be the primary candidates for use in VWC estimation. However, to avoid overlooking other possible indices, a full range of potential band combinations will be evaluated before focusing on a few candidates.

In order to develop relationships between MODIS-based VIs and VWC and to assess the performance of these in estimation, VWC data obtained by ground sampling during SMEX02 (Anderson et al., 2004; Chen et al., 2003; Jackson et al., 2004) and Landsat data are utilized. The corn and soybeans fields within the SMEX02 site are typically 800 m in length. Therefore, the coarse spatial resolution of MODIS can result in the observation of mixed pixels consisting of corn and soybeans fields or different management practices of the same crop. As a result it was necessary to develop a procedure to identify and remove mixed pixels from analyses. Comparisons between MODIS- and Landsat-derived results are conducted at both the field level and regional level. Temporal variations of reflectance and VIs are examined. The relationships between MODIS-derived NDWIs and ground measured VWC are established and evaluated.

2. Data sources and processing

2.1. Data sources

The Walnut Creek watershed (WC) is located just south of Ames, Iowa, USA. It was the focus of SMEX02, which took place from mid-June to mid-July 2002. Within the WC shown in Fig. 1, corn and soybeans occupied 73.4% of the total area (39.5% in corn and 33.9% in soybeans), with an additional 12% in urban and roads, 14% in grasses and

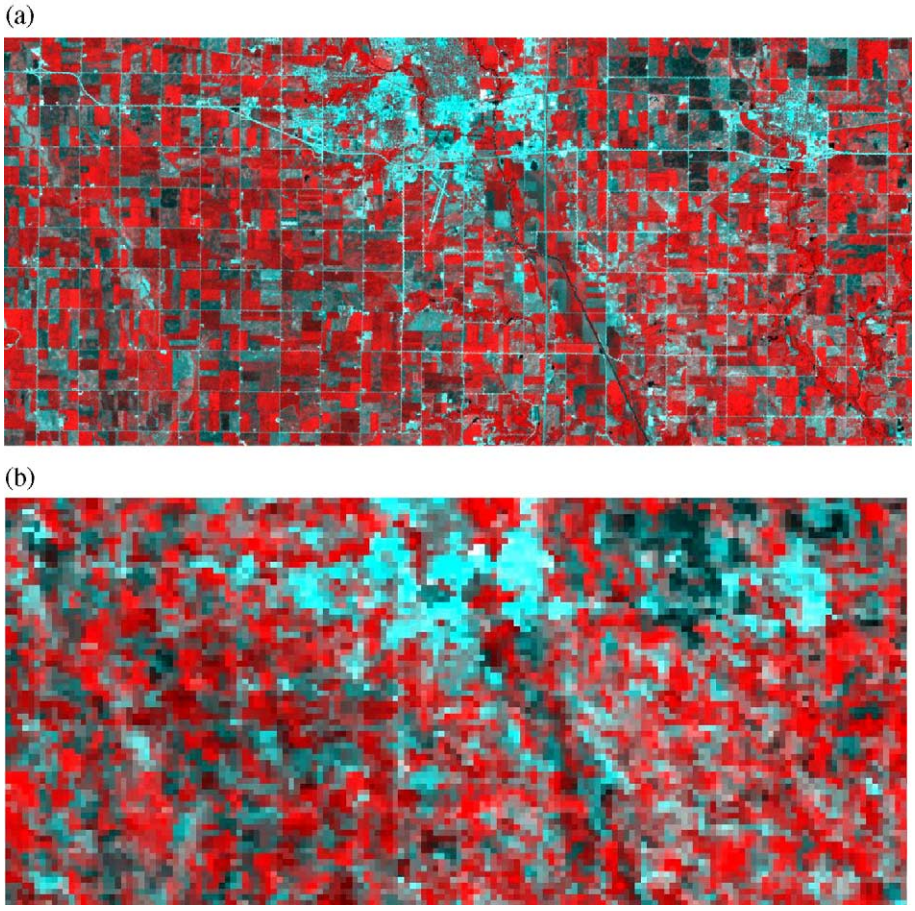

Fig. 1. False-color-composite image of the Walnut Creek watershed during SMEX02 on July 1, 2002 (36.0 × 15.9 km): (a) Landsat TM/ETM (30 m, 4-3-5); (b) MODIS (250 m, 2-1-1).

trees, 0.6% in trace pixels of other classes (Doraiswamy et al., 2004).

Significant changes occurred in the grass and forest classes in May 2002. In early June, corn was still in its early stages of growth and most soybeans fields were essentially bare soil. By the end of June, corn vegetation water content had reached a range between 3 and 4 kg/m^2, while soybeans had values less than 1 kg/m^2. The corn tasseling growth stage began during the first week of July. Soybeans got their first pod at the same time. Soybeans fully bloomed after the second week of July. According to ground based VWC measurements, the VWC of soybeans was nominally 1.5 kg/m^2 and was up to 6.0 kg/m^2 (Anderson et al., 2004; Chen et al., 2003; Jackson et al., 2004). VWC values used in this study are total VWC including both leaf water content and stem water content.

VWC sampling data were available for 31 WC sites: 21 corn fields and 10 soybean fields. Details of the sampling method can be found in Anderson et al. (2004). The sampling time frame encompassed the period from emergence to tasseling/full bloom for corn/soybeans. Sampling locations were selected in advance using photography so that soil and canopy conditions would be homogeneous in the surrounding area on scales of tens of meters, and also where the vegetation appeared healthy and capable of surviving through the experiment (Anderson et al., 2004). The temporal pattern of VWC for individual corn and soybeans fields during SMEX02 is presented in Anderson et al. (2004). Sampling results showed that VWC increased continuously over the entire period as expected. Some sites were sampled twice but most only once during SMEX02.

The SMEX02 study area in Iowa was located on both path 26 and 27 of row 31 of Landsat data. Over the SMEX02 period of primary interest, there were good quality images available on five days: June 7, June 23, July 1, July 8, and July 17. All of these were Landsat 7 except June 23, which was Landsat 5. The image data sets were atmospherically corrected using Second Simulation of the Satellite Signal in the Solar Spectrum model (6S) (Vermote et al., 1997). Further validation of the reflectance corrections was achieved by means of comparison with ground based spectrometer measurements (Chen et al., 2003; Jackson et al., 2004). This high spatial resolution data set was very useful in the present study of MODIS data.

The Terra-MODIS Surface Reflectance Product (MOD09) data were obtained directly from the Land Processes Distributed Active Archive Center of United States Geological Survey (USGS) (http://edcimswww.

cr.usgs.gov/pub/imswelcome/). This product is computed from the MODIS Level 1B data that has been radiometrically corrected, geo-located and sensor SWIR bands electrical crosstalk corrected (Xiong et al., 2004). The product provides an estimate of the surface spectral reflectance for each band, as it would have been measured at ground level if there were no atmospheric scattering or absorption. The algorithm generating this product is based on input from other bands and products and corrects for the effect of atmospheric gases, aerosol, and thin cirrus clouds (Vermote & Vermeulen, 1999). Version 4 of Terra-MODIS surface reflectance (MOD09), which is validated and atmospherically corrected with the best data quality to date, was downloaded and utilized in this study. MODIS data in HDF format downloaded with SIN projection were then reprojected to GeoTIFF files with UTM projection using the MODIS Reprojection Tool (MRT). QA flags of MODIS data, which tell the quality level of the images by use of digital indicators in checking cloud status of the study area with the ability to identify if atmospheric corrections are performed or not, were examined using the MODIS Land Data Operational Product Evaluation (LDOPE) software. Both MRT and LDOPE can be obtained from the USGS website (http://edcdaac.usgs.gov/tools/modis/).

2.2. Data processing

The spatial variation scales of the MODIS data in the SMEX02 region were examined using semi-variograms (Chen & Brutsaert, 1998). The range of the semi-variograms retrieved was around 1500 m. This parameter represents the repeatability of spatial patterns on the image relevant to the typical size of a single corn or soybeans field (See Fig. 2a). Given the study area where corn and soybean are evenly distributed next to each other in most areas, the range becomes approximately twice the typical crop field size (~800 m). Results indicated that the change in the reflectance of a single crop field could be detected by the MODIS data at 250 and 500 m, at least to distinguish the boundaries with mixed crops coverage and the centers of the crop fields. This has been confirmed by visual observations of the crop fields in MODIS images. Thus, it was decided that the MODIS bands 1–7 at 250 and 500 m could be used to identify individual fields. Each sampled field included 10–20 MODIS pixels (See Fig. 2b).

Cloud and shadow pixels were identified using QA flags. The MODIS image on June 6 was used to identify forest/grasses areas since the forest/grasses areas had unique spectral reflectance in early June. The NDVI map developed

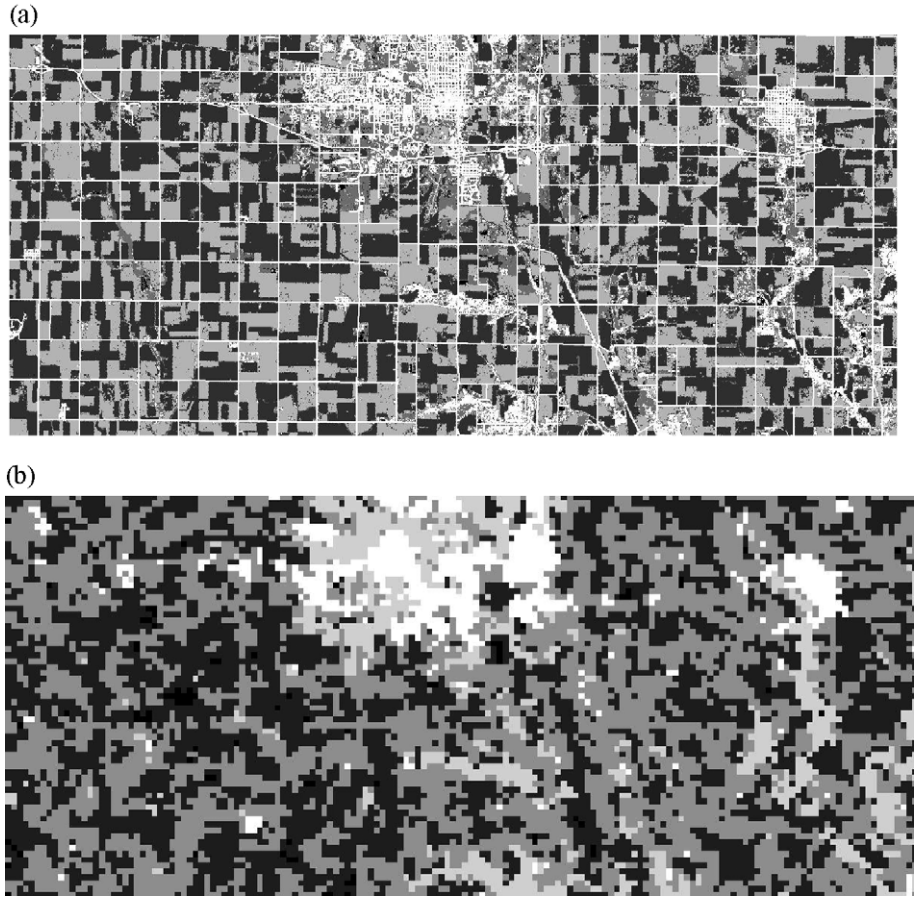

Fig. 2. Classification maps of the Walnut Creek watershed. (a) Supervised Landsat TM/ETM based on field survey (30 m, July 1, 2002); (b) Unsupervised MODIS (250 m, July 1, 2002).

Fig. 3. Corn percentage map (MODIS 250 m) (The darker the color, the higher the corn percentage).

for July 31 was used to identify urban/roads because the NDVI of urban areas and roads were significantly lower than other classes at this time due to canopy cover. The unsupervised MODIS classification map for July 1 is shown as Fig. 2b and can be compared to the 30 m resolution Landsat-based classification map in Fig. 2a. The 30 m land cover classification was performed using a supervised procedure in which training site visits and map digitization are also used (Doraiswamy et al., 2004). As a consistency check, the higher resolution map (Fig. 2a) was resampled to a 250 m resolution and compared to the MODIS product (Fig. 2b). The comparison revealed that 80% of the crop pixels were correctly classified. Considering that an unsupervised procedure was used to classify the MODIS data and that it has a spatial resolution of 250 m, this level of performance is acceptable.

Since one MODIS 250 m pixel covers approximately sixty Landsat 30 m pixels, it is quite possible that MODIS pixels at the edge of a field may include portions of an adjacent field. These could have the same crop or a different crop and/or management practice. Such pixels are defined as mixed pixels. For analyses involving ground and satellite data comparisons, it is essential that these pixels are not used. According to QA flag interpretation, the adjacency effect that accounts for the interchange of radiance between adjacent pixels in heterogeneous landscape due to the sensor point spread function (PSF) (Huang et al., 2002; Qiu et al., 2000) has not been corrected to date in the MOD09 products (Vermote et al., 2002). However, this effect is less significant for medium or low spatial resolution sensor such as MODIS (Huang et al., 2002; Ouaidrari & Vermote, 1999).

Identifying mixed pixels requires the precise matching of the MODIS and Landsat imagery. Therefore, additional verification of geolocation accuracy was performed. Correlations of the spatial patterns between a Landsat image (Fig. 1a) and an equivalent MODIS 'window' (resampled to 30 m) were calculated over a dozen of areas in the image to find an optimal shift, which was 3-pixels (90 m) west and 1-pixel (30 m) south.

Based on this precise geolocation analysis, a 'percentage mapping' approach was used to identify mixed pixels and exclude them from VI calculations. Knowing the percentage of the Landsat corn/soybeans pixels in each corresponding MODIS pixel, percentage maps of corn and soybeans were generated. The corn percentage map is shown in Fig. 3. Only those MODIS pixels with a corn percentage >90% were identified as 'pure' corn, which was 50.3% of all pixels identified as corn in Fig. 2b. As shown in Fig. 3, the pure pixels were concentrated in the central area of each crop field. Only the pure corn/soybeans pixels were used in further calculations.

Fig. 4 illustrates the improvements that can be achieved in estimating corn NDWI using the approach described above to solve the mixed pixel problem. In general, the processed NDWI data show the saturation phenomena more clearly. The overall increase in the level of the curves is the result of eliminating soybean field contributions that have relatively higher reflectance in the SWIR (1640 nm) band used in VI computations (see Fig. 6). The net effects of the geolocation correction and the removal of mixed pixels are

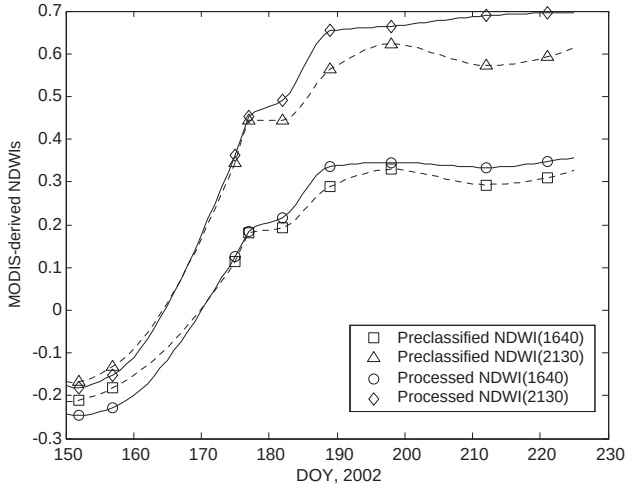

Fig. 4. Comparisons of MODIS-derived $NDWI_{1640}$ $NDWI_{2130}$ for corn before and after geolocation correction and the removal of mixed pixels.

Table 1
R^2 (coefficient of determination) values for different MODIS bands combination of vegetation indices in corn/soybeans VWC estimation linear regressions (R^2 for corn are in bold and shaded; R^2 for soybeans are in italic and not shaded)

MODIS bands		VIS			NIR		SWIR	
	Wavelength	470 nm	555 nm	648 nm	858 nm	1240 nm	1640 nm	2130 nm
VIS	470 nm	–	0.43	0.014	**0.65**	0.61	0.48	0.21
	555 nm	*0.24*	–	0.56	**0.73**	0.69	0.047	0.38
	648 nm	*0.0036*	*0.41*	–	**0.78**	0.69	0.41	0.054
NIR	858 nm	*0.23*	*0.33*	*0.46*	–	0.68	**0.74**	**0.72**
	1240 nm	*0.20*	*0.22*	*0.51*	*0.49*	–	0.54	0.54
SWIR	1640 nm	*0.03*	*0.20*	*0.21*	*0.20*	*0.60*	–	0.52
	2130 nm	*0.28*	*0.58*	*0.28*	*0.54*	*0.56*	*0.54*	–

evident in the correlation (R^2) between the bands/VIs and VWC in Tables 1 and 2. R^2 values were higher (0.57 versus 0.32) for the MODIS NIR (858 nm) after adjustment, since the NIR (858 nm) has distinctly different responses for corn and soybeans. The R^2 values for the NIR (1240 nm) and the SWIR (1640 nm and 2130 nm) relationships were not sensitive to the corrections because in these bands the reflectance values of corn and soybeans are similar.

It is worth noting that, when the typical size of the crop fields (~800 m) is compared to the MODIS resolution (250 or 500 m), any further geolocation correction (90 and 30 m) might not have a large impact on the final results. This is consistent with the statements about the effectiveness of geolocation correction in MODIS L1B products (Barbieri, 1997). Therefore, it was concluded that the removal of mixed pixels was more important than geolocation in reducing error.

For real applications without fully processed Landsat images as references, alternative ways need to be explored to solve the mixed pixel problem. If a classification map is accessible, the procedures described above can be adopted.

3. Results

MODIS- and Landsat-derived surface reflectance data were compared at both the field-averaged level and regional-averaged level to examine the difference between the two satellites as well as the difference between crop species. The same comparisons were conducted for NDWIs. Relationships between SWIR-based NDWIs and VWC were developed and evaluated.

3.1. Comparison of field-averaged MODIS and Landsat reflectance and VI data

In Chen et al. (2003) and Jackson et al. (2004), Landsat pixel values located close to ground sampling sites were related to VWC. MODIS spatial resolution (250–500 m) is quite different from Landsat (30 m) and, therefore, this type of comparison may not be reliable. The basis of analysis in this section will be field averages computed by averaging all ground samples in a field and comparing them to the average of all MODIS pixels in the same field. Characteristics of MODIS and Landsat reflectance and VIs are compared.

Since there were more MODIS data sets than Landsat, the limited Landsat reflectance images were interpolated (cubic polynomial) between dates to generate images for MODIS coverage dates. A maximum value compositing (MVC) may be a useful alternative but the rapid crop growth makes the interpolation method a better choice. Geometric correction, as described previously, was performed for each of these dates. Fig. 5 is a plot of the field-averaged values derived from the Landsat and MODIS data.

Fig. 5a shows the reflectance values for the individual corn fields. The MODIS-derived NIR (858 nm) and SWIR (1640 nm) reflectance values tend to be higher than Landsat

Table 2
Summary of linear regression statistics for estimating VWC from vegetation indices in SMEX02 (R^2: coefficient of determination; σ: root-mean-square error; A: intercept; B: slope)

Y	X	A	B	R^2	σ	A	B	R^2
		(After geolocation correction and mixed pixels removal)				(Before geolocation correction and mixed pixels removal)		
Corn VWC	Landsat-derived $NDWI_{1640}$	7.88	0.58	0.84	0.46	–	–	–
Corn VWC	MODIS-derived $NDWI_{1640}$	9.44	1.37	0.74	0.58	9.12	1.33	0.62
Corn VWC	MODIS-derived $NDWI_{2130}$	6.67	0.10	0.72	0.65	5.66	0.51	0.60
Corn VWC	Landsat-derived NDVI	13.18	−7.47	0.72	0.60	–	–	–
Corn VWC	MODIS-derived NDVI	13.79	−7.07	0.78	0.53	10.89	−4.81	0.66
Soybeans VWC	MODIS-derived $NDWI_{1640}$	1.78	0.28	0.52	0.16	1.48	0.31	0.40
Soybeans VWC	MODIS-derived NDVI	2.06	−0.86	0.46	0.22	2.06	−0.86	0.46

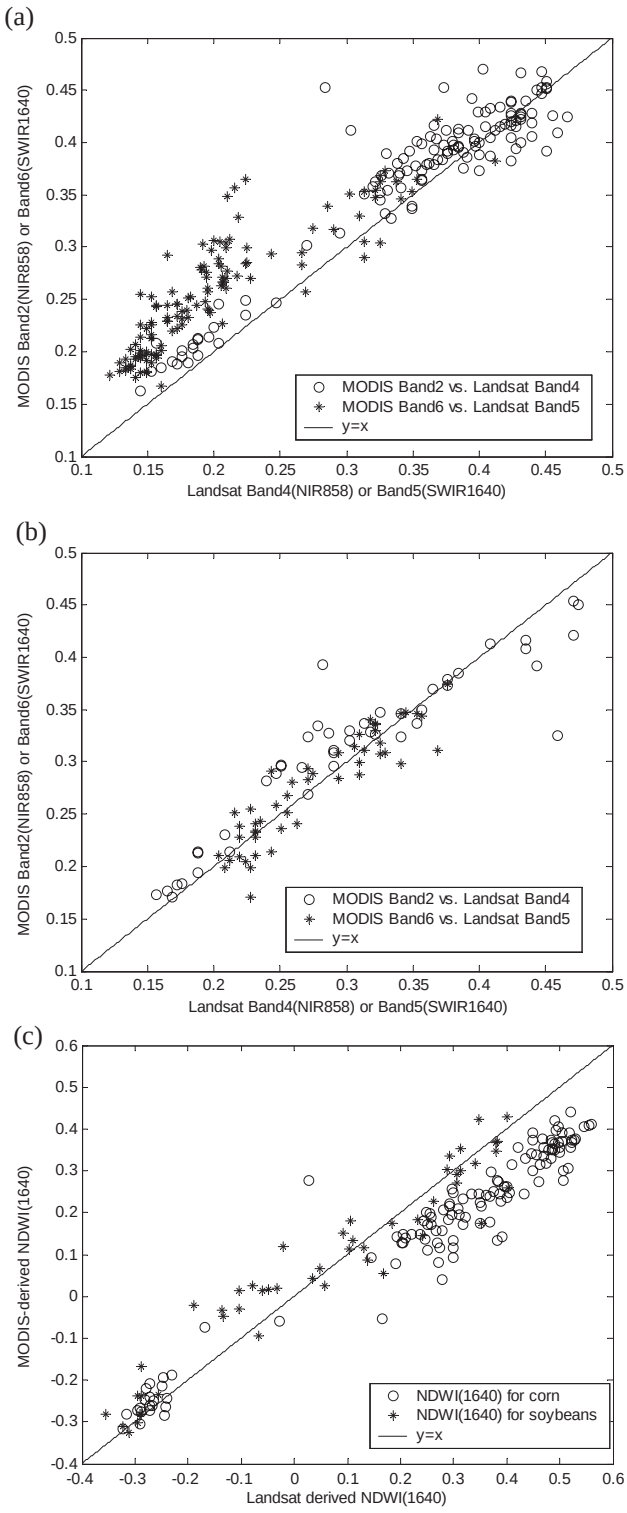

Fig. 5. Comparison of Landsat TM/ETM- and MODIS-derived field-averaged reflectance and $NDWI_{1640}$: (a) NIR and SWIR for corn; (b) NIR and SWIR for soybeans; (c) $NDWI_{1640}$ for corn and soybeans.

values. This could result in a 6% reduction in the MODIS-derived NDVI and an approximately 10% reduction in the MODIS-derived $NDWI_{1640}$ (See Fig. 8a). For soybeans, the Landsat- and MODIS-derived NIR and SWIR reflectance values match each other on most days. Overall in Fig. 5c, we observed very good correlations of the NDWIs derived from the two satellites for soybeans but for corn the Landsat values were biased high, for high values of NDWI. This result could be associated with spatial scale or bandwidth differences of the two sensors.

Further analysis was conducted using regional averages computed by averaging all corn or soybean field values derived above. Insights on the potential of various bands and indices are possible by analyzing this data. Temporal variations of surface reflectance are compared in Fig. 6 for the Red, NIR and SWIR bands on two satellites (MODIS bands 1, 2, 5, 6, 7 and Landsat bands 3, 4, 5). Cubic polynomial regression trendlines are also plotted. The differences between MODIS and Landsat at the field scale we noted above are confirmed here.

The Landsat-derived surface reflectance curves in Fig. 6 exhibit smooth temporal patterns. Deviations are seen in the MODIS data. Such phenomenon is attributable to the persistence of cloud/shadow effects in some pixels on unclear dates and the resolution and bandwidth difference of

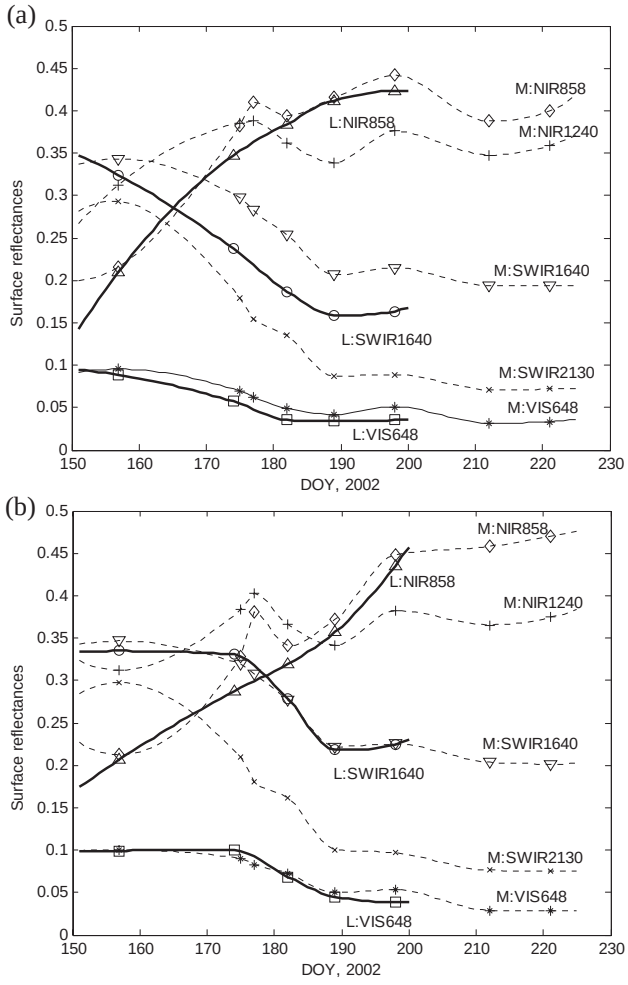

Fig. 6. Temporal variations of regional-averaged surface reflectance for different bands: a) Corn; b) Soybeans. (L: Landsat TM/ETM bands in solid lines; M: MODIS bands in dot lines.)

MODIS sensors compared to Landsat sensors. However, the curves for VIs shown in Fig. 8 are smooth for both satellites. This reduction in variability for the MODIS indices might indicate that the source of variation observed in the reflectance data is present in all bands and is normalized in computing the VI.

3.2. Responses of the spectral bands to vegetation growth

Results presented in Zarco-Tejada et al. (2003) and Ceccato et al. (2002a) using the PROSPECT model suggested that the surface reflectance in the reflective infrared bands (700–3000 nm) is affected by Chlorophyll, dry matter and leaf structure, in addition to vegetation water content. Soil effects can also contribute to the surface reflectance, especially for sparsely vegetated area. Therefore, it is of interest to see if there are any distinct patterns in these bands as the crops grow.

In Fig. 6, both the Landsat and the MODIS data showed clear temporal trends of surface reflectance for different bands. During the vegetation growing period, the NIR (858 nm) bands increase, but values for the SWIR bands decrease, which is a clear indication of strong water absorption. The RED (648 nm) also decreases due to its correlation with vegetation pigment, dry biomass and leaf structure.

Since crop coverage measurements were available from SMEX02, a simple mixture model was employed to remove the soil effect and achieve a 'pure' vegetation reflectance as if the pixel was fully covered by the crops (Jasinski, 1996; Townshend et al., 2000). Fig. 7 shows the averaged gradients for linear relationships between reflectance and time for the period (DOY160-189) before and after the soil effect correction for both MODIS and Landsat. The results show that the two satellites agree for the NIR (858 nm) and the SWIR (1640 nm). In Fig. 7, the gradient of the NIR (1240 nm) and the SWIR bands departed show more sensitivity to VWC once the soil effect was removed, this

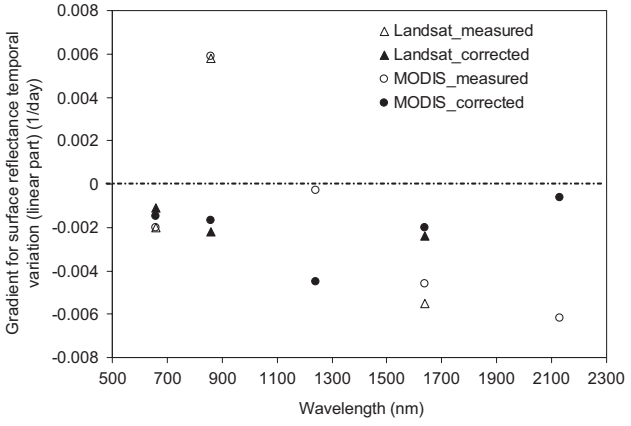

Fig. 7. Comparisons of the gradient of the linear temporal variation part (DOY160–189) of the reflectance from each band before and after soil effect correction (SMEX02, corn).

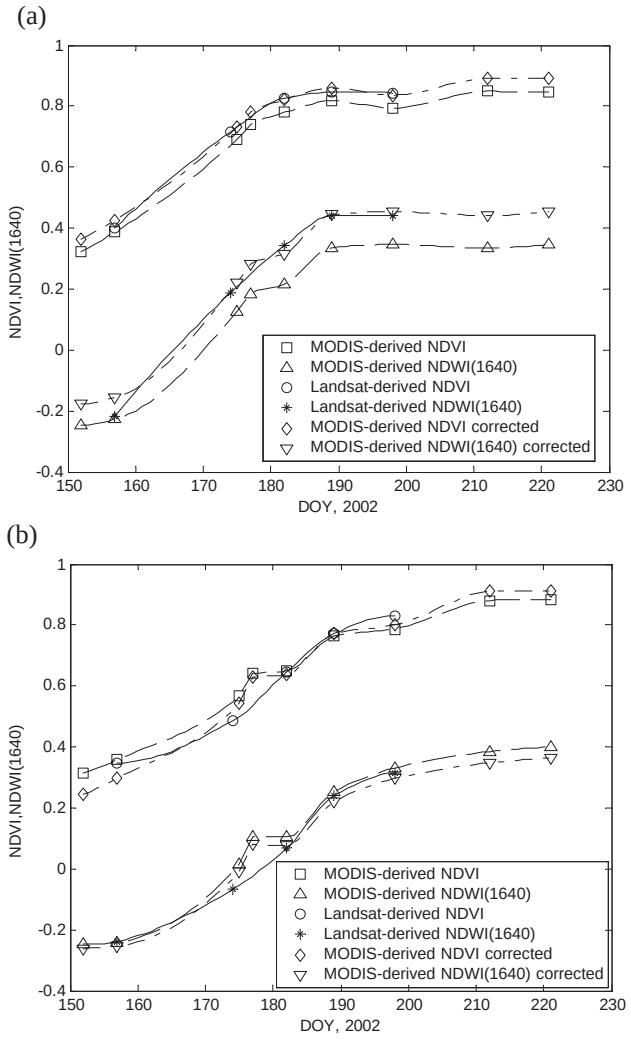

Fig. 8. Landsat TM/ETM- and MODIS-derived regional-averaged NDVI and $NDWI_{1640}$ after interpolation and minimum deviation correction: a) Corn ($NDWI_{1640}$(Landsat) = 1.063 * $NDWI_{1640}$(MODIS) + 0.086; NDVI(Landsat) = 1.011 * NDVI(MODIS) − 0.034); b) Soybeans ($NDWI_{1640}$(Landsat) = 0.962 * $NDWI_{1640}$(MODIS) − 0.022; NDVI(Landsat) = 1.063 * NDVI(MODIS) − 0.124).

demonstrates that the NIR (124 nm) and SWIR bands respond to vegetation growth more well under full vegetated conditions, which agrees with Gao (1996) about the NIR (1240 nm).

In order to apply the NIR (1240 nm) and SWIR bands for VWC estimation in partially vegetated areas some knowledge of the vegetation coverage is needed to account for soil effects. In practice, vegetation coverage information is not easy to obtain, which makes VWC estimation difficult. Although vegetation index bands combination is believed to effectively reduce leaf structural effect, however, the other effects from dry matter and soil background contamination may persist. In such cases, the SWIR bands which are more water absorption dominated may be more potentially useful for VWC estimation minimizing other effects. Further scientific studies are necessary to examine the extent of the utilization of the NIR (1240 nm) in VWC estimation.

3.3. Saturation in MODIS-derived VIs

As discussed in Chen et al. (2003) and Jackson et al. (2004), the Landsat $NDWI_{1640}$ lagged the NDVI in corn fields by one week in SMEX02. However, that analysis only used data through DOY198. In the present study, MODIS data through DOY220 were available, which allowed the examination of saturation for an extended period for corn and soybeans. Fig. 8a shows that the MODIS-derived NDVI and NDWI for corn saturated between DOY198 and DOY220. For soybeans fields, saturation did not occur during the Landsat analysis. As shown in Fig. 8b, using the MODIS data, saturation for the NDVI occurred near DOY202 and for the NDWIs near DOY212, a lag of about 10 days between the two types of VIs. This demonstrated that the saturation occurred to both corn and soybeans, but at different times.

3.4. Evaluation of VI candidates for corn VWC estimation

Ground observations of VWC collected during SMEX02 are used here to evaluate the potential applications of satellite remotely sensed reflectance for VWC estimation. For all sample fields, cubic polynomial data interpolation was used with data from days with VIs to estimate values on all dates with ground observations. A systematic evaluation is conducted for each of the 7 bands. The first step in this process was the examination of the relationship between VWC and reflectance for each band. Although there are many alternative nonlinear models that might be used, based upon preliminary studies and for the purposes of simplification, we chose to use a linear model as our basis of comparison for the various band combinations. This may not apply to the entire growth cycle, however, a linear relationship between VWC and NDWI was found to be

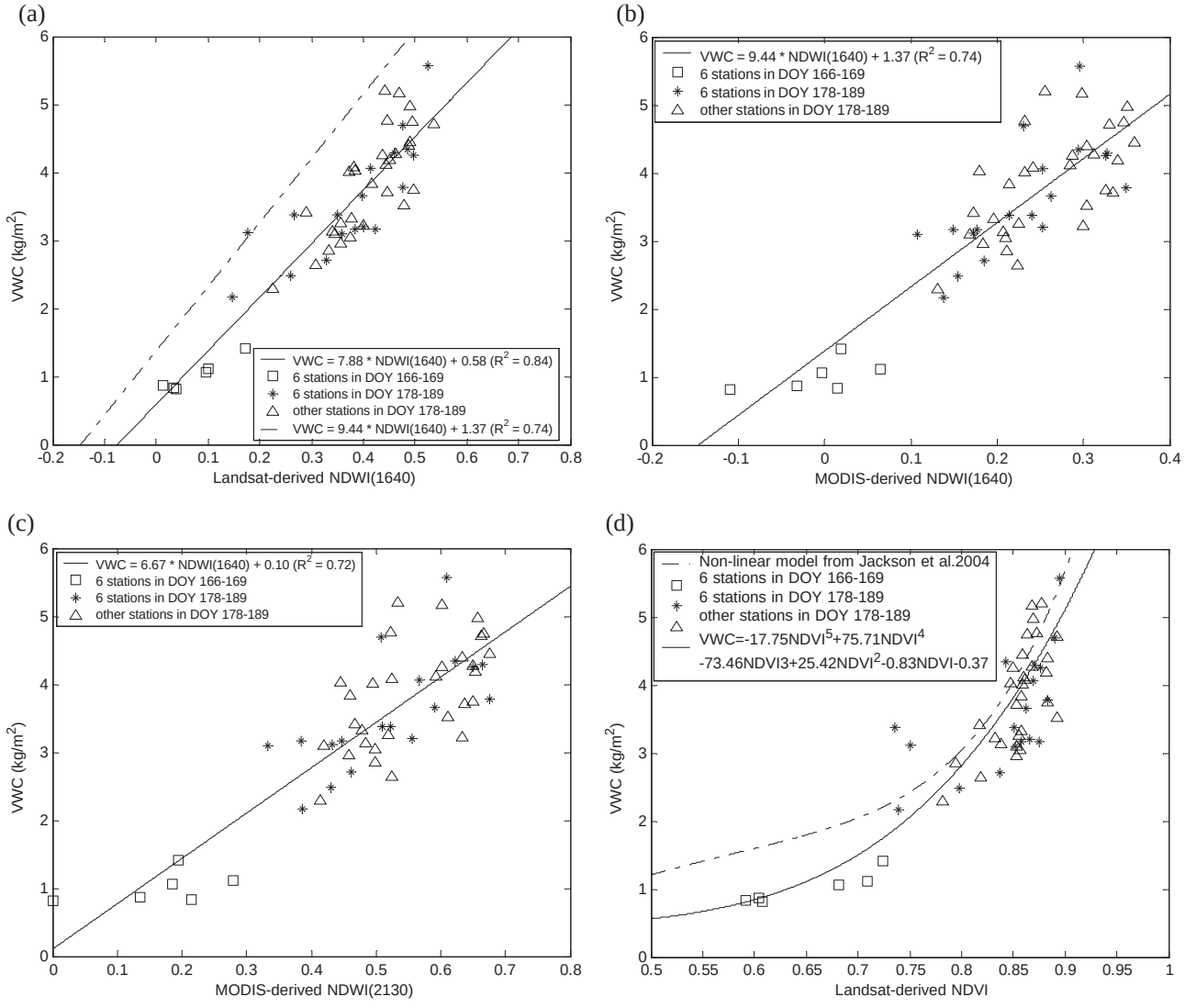

Fig. 9. VWC estimation for corn: (a) Linear VWC estimation using Landsat TM/ETM-derived $NDWI_{1640}$; (b) Linear VWC estimation using MODIS-derived $NDWI_{1640}$; (c) Linear VWC estimation using MODIS-derived $NDWI_{2130}$; (d) Non-Linear VWC estimation using Landsat TM/ETM-derived NDVI.

applicable in Chen et al. (2003) and Jackson et al. (2004) for the periods between DOY155 and DOY189. Saturation was observed at a later stage of this period for NDVI but with one-week lag in the case of NDWI. Here we used only this linear period.

Further examination of the R^2 values in Table 1 results in several interesting observations. First of all, the 7 bands are grouped together into three categories: VIS, NIR and SWIR.

- Inter-category combinations yield low R^2 values generally in each of the VIS, NIR and SWIR categories.
- Cross-category combination between VIS and SWIR also yields low R^2.
- The combinations with the NIR (858 nm) band have resulted into high R^2 (>0.7) of 0.73, 0.78, 0.74 and 0.72 with VIS bands (555 and 648 nm) and SWIR bands (1640 and 2130 nm) respectively. These combinations seem to be the best candidates for VWC estimation and they are indeed the previously discussed NDVIs and NDWIs.

In fact, there are similarities within in each category. For example, the saturation phenomenon of $NDVI_{648}$ (or simply NDVI as in Eq. (3)) is also observed for $NDVI_{555}$. It is also expected that the similarity that exists in $NDWI_{1640}$ is also observed in $NDWI_{2130}$. Based on the above observations, the NDVIs and the NDWIs are the combinations with the highest correlation of corn VWC. Finally, the advantage of $NDWI_{1640}$ is justified by the fact that the saturation at the end of the corn growth occurred one week later than NDVI (Chen et al., 2003; Jackson et al., 2004). For VWC estimation, the SWIR bands appear to be most useful. The NIR bands are complementary to it. For example, the NIR (858 nm) band is a good reference for VIs because the two best VIs (NDVI and NDWI) are based on it.

The above discussions are purely based on corn VWC data. Since the soybean VWC is much lower than corn VWC, the satellite VIs are not sensitive enough to show the performance of different band combinations so it will not be discussed further.

3.5. VWC estimation using VIs

Relationships between the VIs and VWC were developed and then evaluated by plotting VI and VWC data in Figs. 9 and 10. Also shown in these plots are the linear regression lines. The R^2 values and other variables of linear regression equations used for VWC estimation with the VIs are listed in Table 2. The results are in general agreement with those reported in Chen et al. (2003) and Jackson et al. (2004). The Landsat-derived NDWI achieved the highest correlation coefficient $R^2=0.84$ and the smallest root-mean-square error 0.46 kg/m^2. The root-mean-square errors of the MODIS-derived $NDWI_{1640}$ and $NDWI_{2130}$ are 0.58 and 0.65 kg/m^2 respectively, which are approximately 10% of the observed VWC range (5.5 kg/m^2).

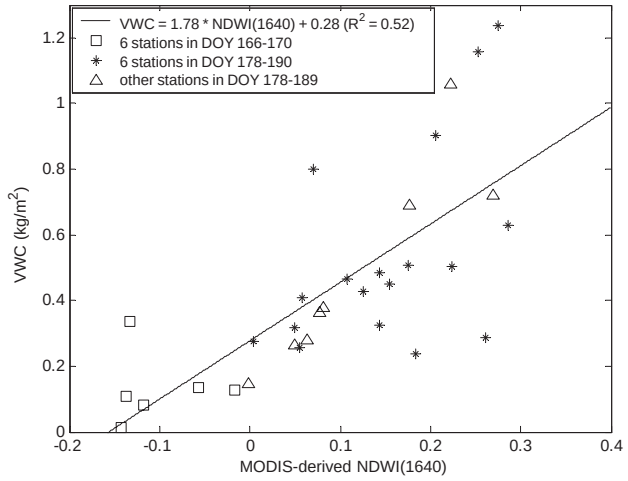

Fig. 10. VWC estimation for soybeans: Linear VWC estimation using $NDWI_{1640}$.

These results confirm that using the MODIS-derived NDWIs to estimate VWC will have slightly lower but comparable accuracy to using Landsat-derived VIs for corn. It was noted that the MODIS-derived NDVI appeared to be slightly better than the Landsat-derived (0.78 versus 0.72 in R^2 values). In reviewing the NDVI data (Fig. 9d), it appears that this may be associated with nonlinearity in the relationship between these variables. Based solely on root-mean-square errors the NDVI also performed well. But because of the saturation at high VWC (Fig. 9d) the conclusion from Chen et al. (2003) and Jackson et al. (2004) on the superiority of the NDWI over the NDVI remains valid.

As shown in Fig. 10 for soybeans, the VWC values are much lower, typically in the range of 0 to 1.3 kg/m^2. These results are consistent to those of Chen et al. (2003) and Jackson et al. (2004).

4. Discussion and conclusions

This study using MODIS data has explored the possible use of MODIS reflectance data for the estimation of VWC. Using corn and soybeans, vegetation indices (NDVI, NDWIs) were derived from MODIS and Landsat over the Walnut Creek watershed in Iowa, USA during the SMEX02 study (mid-June to mid-July, 2002). Red, NIR and SWIR bands were used for VIs calculations.

MODIS images were processed before VI calculations. This included refined geolocation correction using available Landsat images. Fields with mixed pixels were identified and excluded in VI calculations using a technique developed here. For practical studies using coarse resolution data, mixed pixels could be eliminated to accord with accuracy estimation requirements. This resulted in an improvement in the temporal variation of the VI. After comparing the MODIS spatial resolution to the general spatial scale of fields in the study area, it was noted that the field-averaged

results would be more reliable if each individual crop site was larger. This is a drawback of MODIS in applications involving small or medium sized fields.

Although some variability was observed in the temporal patterns of individual MODIS bands, these seemed to be cancelled in computing the VIs as bands were combined. MODIS-derived VIs displayed smooth temporal variations that were comparable to the Landsat results. Although MODIS has a coarser resolution, these results show the potential for using MODIS data and since it is available much more frequently it may have wider application.

Although MODIS and Landsat agree with each other over the soybeans fields, MODIS observed higher surface reflectance in all spectral bands than Landsat over the cornfields. This may be due to the difference in their sensor bandwidths. The sensitivity of sensor difference to the crop species difference is under investigation.

The saturation of the NDVI and NDWI as corn matures was confirmed from previous studies (Chen et al., 2003; Jackson et al., 2004). A lag of one week for corn NDWI was observed as was a 10 day lag for soybeans. The SWIR-based VIs were found to track the growth pattern better than others.

A simple linear mixture model was used to remove the soil effect and the NIR (1240 nm) and SWIR bands responded to VWC changes for "pure" vegetated area more convincingly. However, obtaining the necessary vegetation coverage information may be impractical. This result suggests that effect from soil background and other vegetation constituents such as dry matter and vegetation structure may limit the ability of those bands for corn VWC estimation. The changes of SWIR (1640 and 2130 nm) were demonstrated to be more strongly related to corn VWC even when soil and other effects exist in addition to vegetation index bands combination mechanism. It was concluded that SWIR bands in the water absorption spectral range as the measuring bands in vegetation indices are useful for corn VWC estimation from operational satellites, as the complements to conventional NDVI.

The availability of ground-based VWC measurements from the SMEX02 made it possible to develop and verify relationships between VIs and VWC. All possible combinations of the 7 MODIS bands have been used to construct vegetation indices, which were evaluated by comparing correlation coefficients with the corn VWC. It was found that NDVIs and NDWIs have the highest correlations and thus are the best candidate VIs for corn VWC estimation. For linear regressions between corn VWC (0–6.0 kg/m^2) and the SWIR-based VIs, the R^2 values were 0.84, 0.74 and 0.72 for Landsat-derived $NDWI_{1640}$, MODIS-derived $NDWI_{1640}$ and $NDWI_{2130}$ respectively. However, linear relationships were not as strong for soybeans, which had relatively low VWC levels (0–1.5 kg/m^2).

This study has demonstrated that VWC can be retrieved using MODIS data for the crops and regions examined. This is a positive step towards the development of more robust techniques based upon a data source that is globally available on a routine basis.

Acknowledgment

The authors are grateful that the Land Processes Distributed Active Archive Center of USGS that provided all MODIS data and SMEX02 data from the NSIDC. The Overseas Research Scholarship (ORS) from Universities UK to support Jingfeng Huang's study and research is sincerely acknowledged as well.

References

Anderson, M. C., Neale, C. M. U., Li, F., Norman, J. M., Kustas, W. P., Jayanthi, H., et al. (2004). Upscaling ground observation of vegetation water content, canopy height, and leaf area index during SMEX02 using aircraft and Landsat imagery. *Remote Sensing of Environment*, *92*, 447–464.

Barbieri, R. (1997). *MODIS level 1B algorithm theoretical basis (ATB MOD-01), Version 2, February, 1997* (http://modis.gsfc.nasa.gov/data/atbd/atbd_mod01.pdf)

Bull, C. R. (1991). Wavelength selection for near-infrared reflectance moisture meters. *Journal of Agricultural Engineering Research*, *49*, 113–125.

Ceccato, P., Flassee, S., Tarantola, S., Jacquemoud, S., & Gregoire, J.-M. (2001). Detecting vegetation leaf water content using reflectance in the optical domain. *Remote Sensing of Environment*, *77*, 22–33.

Ceccato, P., Gobron, N., Flasse, S., Pinty, B., & Tarantola, S. (2002a). Designing a spectral index to estimate vegetation water content from remote sensing data: Part 1. Theoretical approach. *Remote Sensing of Environment*, *82*, 188–197.

Ceccato, P., Flasse, S., & Gregoire, J. (2002b). Designing a spectral index to estimate vegetation water content from remote sensing data: Part 2. Validation and applications. *Remote Sensing of Environment*, *82*, 198–207.

Chen, D., & Brutsaert, W. (1998). Satellite-sensed distribution and spatial patterns of vegetation parameters over tall grass prairie. *Journal of Atmospheric Sciences*, *55*, 1225–1238.

Chen, D., Jackson, T. J., Li, F., Cosh, M. H., Walthall, C., & Anderson, M. (2003). Estimation of vegetation water content for corn and soybeans with a Normalized Difference Water Index (NDWI) using Landsat Thematic Mapper data. *Proceeding of International Geosciences and Remote Sensing Symposium, 2003 (IGARSS'03)* (pp. 2853–2856). New York, USA: Institute of Electrical and Electronics Engineers.

Doraiswamy, P., Hatfield, J., Jackson, T., Akhmedov, B., Prueger, J., & Stern, A. (2004). Crop condition and yield simulation using Landsat and MODIS. *Remote Sensing of Environment*, *92*, 548–559.

Fourty, T., & Baret, F. (1997). Vegetation water and dry matter contents estimated from top-of-the-atmosphere reflectance data: A simulation study. *Remote Sensing of Environment*, *61*, 34–35.

Gamon, J. A., Field, C. B., Goulden, M. L., Griffin, K. L., Hartley, A. E., Joel, G., et al. (1995). Relationships between NDVI, canopy structure, and photosynthesis in three Californian vegetation type. *Ecological Applications*, *5*, 28–41.

Gao, B. (1996). NDWI—a normalized difference water index for remote sensing of vegetation liquid water from space. *Remote Sensing of Environment*, *58*, 257–266.

Gao, B. C., & Goetz, A. F. H. (1995). Retrieval of equivalent water thickness and information related to biochemical components of vegetation canopies from AVIRIS data. *Remote Sensing of Environment*, *52*, 155–162.

Huang, C., Twonshend, J., Liang, S., Kalluri, S., & DeFries, R. (2002). Impact of sensor's point spread function on land cover characterization: Assessment and deconvolution. *Remote Sensing of Environment*, *80*, 203–212.

Hunt Jr., E. R., & Rock, R. N. (1989). Detection of changes in leaf water content using near- and middle-infrared reflectance. *Remote Sensing of Environment*, *30*, 43–54.

Hunt Jr., E. R., & Running, S. W. (1990). Problems with leaf water relations to regional scales. *Proceedings of IGRASS '90* (pp. 1259–1261). New York, USA: Institute of Electrical and Electronics Engineers.

Jackson, T. J., Chen, D., Cosh, M., Li, F., Anderson, M., & Walthall, C., et al. (2004). Vegetation water content mapping using Landsat data derived normalized difference water index for corn and soybeans. *Remote Sensing of Environment*, *92*, 475–482.

Jasinski, M. F. (1996). Estimation of subpixel vegetation density of natural regions using satellite multispectral imagery. *IEEE Transactions on Geoscience and Remote Sensing*, *34*, 804–813.

Ouaidrari, H., & Vermote, E. F. (1999). Operational atmospheric correction of Landsat TM data. *Remote Sensing of Environment*, *70*, 4–15.

Penuelas, J., Filella, I., Biel, C., Serrano, L., & Save, R. (1993). The reflectance at the 950–970 mm region as an indicator of plant water status. *International Journal of Remote Sensing*, *14*, 1887–1905.

Pu, R., Ge, S., Kelly, N. M., & Gong, P. (2003). Spectral absorption features as indicators of water status in coast live oak (*Quercus agrifolia*) leaves. *Journal of International Remote Sensing*, *24*, 1799–1810.

Qiu, S., Godden, G., Wang, X., & Guenther, B. (2000). Satellite-earth remote sensor scatter effects on earth scene radiometric accuracy. *Metrologia*, *37*, 411–414.

Roberts, D. A., Green, R. O., & Adams, J. B. (1997). Temporal and spatial patterns in vegetation and atmospheric properties from AVIRIS. *Remote Sensing of Environment*, *62*, 223–240.

Rollin, E. M., & Milton, E. J. (1998). Processing of high spectral resolution reflectance data for the retrieval of canopy water content information. *Remote Sensing of Environment*, *65*, 86–92.

Serrano, L., Ustin, S. L., Roberts, D. A., Gamon, J. A., & Penuelas, J. (2000). Deriving water content of chaparral vegetation from AVIRIS data. *Remote Sensing of Environment*, *74*, 570–581.

Sims, D. A., & Gamon, J. A. (2002). Estimation of vegetation water content and photosynthetic tissue area from spectral reflectance: A comparison of indices based on liquid water and chlorophyll absorption features. *Remote Sensing of Environment*, *84*, 526–537.

Townshend, J., Huang, C., Kalluri, S., Defries, R., & Liang, S. (2000). Beware of per-pixel characterization of land cover. *International Journal of Remote Sensing*, *21*, 839–843.

Tucker, C. J. (1980). Remote sensing of leaf water content in the near-infrared. *Remote Sensing of Environment*, *10*, 23–32.

Ustin, S. L., Roberts, D. A., Pinzon, J., Jacquemoud, S., Gardner, M., & Scheer, G., et al. (1997). Estimation canopy water content of chaparral shrubs using optical methods. *Remote Sensing of Environment*, *65*, 280–291.

Vermote, E. F., Saleous, N. Z., & Justice, C. O. (2002). Atmospheric correction of MODIS data in the visible to middle infrared: First results. *Remote Sensing of Environment*, *83*, 97–111.

Vermote, E. F., Tanre, D., Deuze, J. L., Herman, M., & Morcrette, J. J. (1997). Second simulation of the satellite signal in the solar spectrum. *IEEE Transactions on Geoscience and Remote Sensing*, *35*, 675–686.

Vermote, E. F., & Vermeulen, A. (1999). *Algorithm technical background document: Atmospheric correction algorithm: Spectral reflectance (MOD09), version 4, April 1999*.

Xiong, X., Chiang, K., Adimi, F., Yatagai, H., & Barnes, W. (2004). MODIS correction algorithm for out-of-band response in the short-wave IR bands. Sensors, systems and next-generation satellites VII. *Proceeding of the International Society for Optical Engineering—Sensors, Systems and Next-generation Satelites VII*, *vol. 5234* (pp. 605–613). Bellingham, WA, USA: the International Society for Optical Engineering.

Zarco-Tejada, P. J., Rueda, C. A., & Ustin, S. L. (2003). Water content estimation in vegetation with MODIS reflectance data and model inversion methods. *Remote Sensing of Environment*, *85*, 109–124.